Journal of Theoretical Biology 362 (2014) 69–74

Contents lists available at ScienceDirect

Journal of Theoretical Biology

journal homepage: www.elsevier.com/locate/yjtbi

Two programmed replicative lifespans of *Saccharomyces cerevisiae* formed by the endogenous molecular-cellular network

Jie Hu [a], Xiaomei Zhu [b], Xinan Wang [c], Ruoshi Yuan [d], Wei Zheng [a], Minjuan Xu [a,*], Ping Ao [a,**]

[a] Key Laboratory of Systems Biomedicine, Ministry of Education, Shanghai Center for Systems Biomedicine Shanghai Jiao Tong University, Shanghai 200240, China
[b] GeneMath, 5525 27th Ave. N.E., Seattle, WA 98105, USA
[c] Department of Computer Science and Engineering, Shanghai Jiao Tong University, Shanghai 200240, China
[d] School of Biomedical Engineering, Shanghai Jiao Tong University, Shanghai 200240, China

ARTICLE INFO

Available online 19 January 2014

Keywords:
Exponential growth
Post-diauxic growth
Pheromone signaling
MAPK
Cell cycle

ABSTRACT

Cellular replicative capacity is a therapeutic target for regenerative medicine as well as cancer treatment. The mechanism of replicative senescence and cell immortality is still unclear. We investigated the diauxic growth of *Saccharomyces cerevisiae* and demonstrate that the replicative capacity revealed by the yeast growth curve can be understood by using the dynamical property of the molecular-cellular network regulating *S. cerevisiae*. The endogenous network we proposed has a limit cycle when pheromone signaling is disabled, consistent with the exponential growth phase with an infinite replicative capacity. In the post-diauxic phase, the cooperative effect of the pheromone activated mitogen-activated protein kinase (MAPK) signaling pathway with the cell cycle leads to a fixed point attractor instead of the limit cycle. The cells stop dividing after several generations counting from the beginning of the post-diauxic growth. By tuning the MAPK pathway, *S. cerevisiae* therefore programs the number of offsprings it replicates.

1. Introduction

Most living cells cannot proliferate indefinitely. “Hayflick Limit” was proposed in the 1960s when it was observed that human diploid cell lines have a limited doubling potential (a clonable cell can only proliferate 50 ± 10 population) (Hayflick, 1965). Mesenchymal stem cells (MSC), a multipotent adult stem cell population, enter replicative senescence after an accumulation of 6–16 population doublings of cells *in vitro* (Wagner et al., 2008). However, human embryonic stem cells (hESCs) cultured *in vitro* can divide infinitely (Zeng and Rao, 2007).

Several explanations for the finite replicative capacity have been proposed. One of them is the telomere-shortening hypothesis. It was found that the length of the telomere can influence the cellular replication (Bodnar et al., 1998; Allsopp et al., 1992; Lundblad and Szostak, 1989). Cellular damage caused by oxidative stress was also proposed as a reason (Lawless et al., 2012; Herker et al., 2004). The accumulation of extrachromosomal rDNA circles (ERCs) and the accumulation of scars were proposed specifically for *Saccharomyces cerevisiae* (Mortimer and Johnston, 1959).

Questions still remain. (1) Considering lifespans of organisms, mammalian aging occurs almost simultaneously with age, e.g., human enters the aging stage around sixties while plants such as Norway spruce (Lamersdorf and Borken, 2004) and reptiles seem not to have a time clock for aging. It is more likely that aging is regulated by an intrinsic molecular mechanism (Blagosklonny and Hall, 2009). Replicative capacity, as one of the most important physiologic and cellular functions, should also be formed by a molecular mechanism rather than telomere or ROS accumulation. (2) “Hayflick Limit” does not seem to be able to account for different replicative capacities of embryonic stem cells and mesenchymal stem cells (Suda et al., 1987; Zeng and Rao, 2007; Wagner et al., 2008). (3) In microbes, the growth of *Escherichia coli* shows the same exponential growth trend in the diauxie phenomenon (Monod, 1949). But the growth of *S. cerevisiae* is different (Stahl et al., 2004). The growth is exponential during the anaerobic phase but non-exponential in the aerobic phase.

In this paper, we demonstrate that the replicative life is determined by the internal organization of the molecular interaction network. A time evolution tendency is given by this network. Specifically, since the cell division and growth are regulated by the

* Corresponding author.
** Co-corresponding author.
E-mail addresses: minjuanxu@sjtu.edu.cn (M. Xu), aoping@sjtu.edu.cn (P. Ao).

0022-5193/$ - see front matter © 2014 Elsevier Ltd. All rights reserved.
http://dx.doi.org/10.1016/j.jtbi.2014.01.007

molecular network, there is a tendency for further division, the cells are more likely to grow continuously. This tendency corresponds to the type of attractors of the network dynamics. If the dynamics of the endogenous network has a limit cycle attractor, the cells are continuously dividing. We can observe an exponential growth of cells from experiments. In case the limit cycle is replaced by a fixed point attractor, the cells will replicate a finite number of times counting from the diauxic shift, leading to the post-diauxic growth.

We propose a programmed replicative lifespan for cells. The gene expression and protein activation levels in a cell, $x_1, x_2, \ldots, x_n$, are a set of time dependent variables $\mathbf{x}(t) = [x_1(t), x_2(t), \ldots, x_n(t)]^\tau$. The continuous dynamics of $\mathbf{x}(t)$ throughout generations of *S. cerevisiae* is governed by the dynamics formed by the endogenous molecular-cellular network (Zhu et al., 2004; Ao et al., 2008; Wang et al., 2013) with given initial conditions. Cell cycle gene expression and protein activation levels are determined in such a manner. While an initial condition for a mother cell is $\mathbf{x}_0$, a daughter cell born at t_b inherits the gene expression and protein activation levels $\mathbf{x}(t_b)$ from its mother cell. Alternatively, if we wish to consider dynamics within one life cycle, then the initial values of $\mathbf{x}(t)$ in mother cell and daughter cell are different. Therefore, the replicative lifespans are different for mother and daughter cells. The replicative capacity for both the mother and daughter cells are determined after an initial condition for mother cells is given. We define the replicative lifespans for this population of cells the programmed replicative lifespan.

To illustrate, *S. cerevisiae* is used as a model organism. Pre-diauxic (exponential) and post-diauxic growths are observed from our experiment. The endogenous network of *S. cerevisiae* with proper initial conditions can build up two programmed replicative lifespans corresponding to these two growth phases. The pre-diauxic program is a cyclic process (Ball et al., 2011). In this case, the cyclin-dependent kinase, Cdc28/Cln3, which promotes G1 to S transition, can be indirectly activated by Sic1, a cyclin-dependent kinase inhibitor. Meanwhile, Cdc28/Cln1, 2 and Swe1 will inhibit Sic1 in return. In this way, cell cycle operates infinitely.

In the post-diauxic program, the metabolism of the yeast dramatically changes, it starts the aerobic respiration to sustain its energy and substance consumption, and the mechanical properties of the yeast, such as the rigidity of the cell membrane, change accordingly, which can be regarded as a new life mode (Ao et al., 2008). In this mode, pheromone as an intercellular mating signal is produced and secreted into environment whose biological significance has been discussed in detail. The genes coding for pheromone production and secretion, like Ste6 (Kuchler et al., 1989), have risen a lot, which has been observed in the microarray data. Activated by pheromone, the mitogen-activated protein kinase (MAPK) signaling pathway that can suppress the activity of the cell cycle network (Kurjan, 1992). We have reconstructed the growth curve of the post-diauxic phase based on such a program.

In the following, we first summarize our main results, including the growth curve of the two phases measured experimentally and the reconstruction of the growth curve based on our hypothesis mathematically. The methods and related materials are discussed in Section 3. Our conclusion is in Section 4.

2. Results

2.1. Two programs of replicative lifespan in yeast growth

The growth curve for *S. cerevisiae* is measured in Fig. 2. Two major phases can be recognized. At the exponential phase, the glycolytic pathway involved genes express higher. Yeast cells proliferate for about 6 h by using a fermentable carbon source (Broach, 2012). The growth curve in Fig. 2(a) can be well fitted with the exponential curve (see Fig. 2(c)). The coefficient of determination $R^2 = 0.9948$. Once the glucose is exhausted Fig. 2 (b), yeast cells cross the diauxic shift (Brauer et al., 2005) and enter the post-diauxic phase. In this phase, the respiration pathway involved genes express higher (Brauer et al., 2005). Yeast cells grow slowly for approximately 30 h by oxidative respiration.

2.1.1. Post-diauxic growth

To reconstruct the growth curve theoretically, we use the following model to describe the time evolution of the total number of yeast $N(t)$ in the post-diauxic growth: Suppose that there are initially N_0 mother yeast cells $N(0) = N_0$. For this population of mother cells, ρ_i $(i = 0, 1, \ldots, [T_s/\Delta T])$ denotes the number of yeast in the population that can divide i times, where T_s is the time for the population reaching stationary; ΔT is the period of cell cycle in this growth stage; $[T_s/\Delta T]$ is the largest

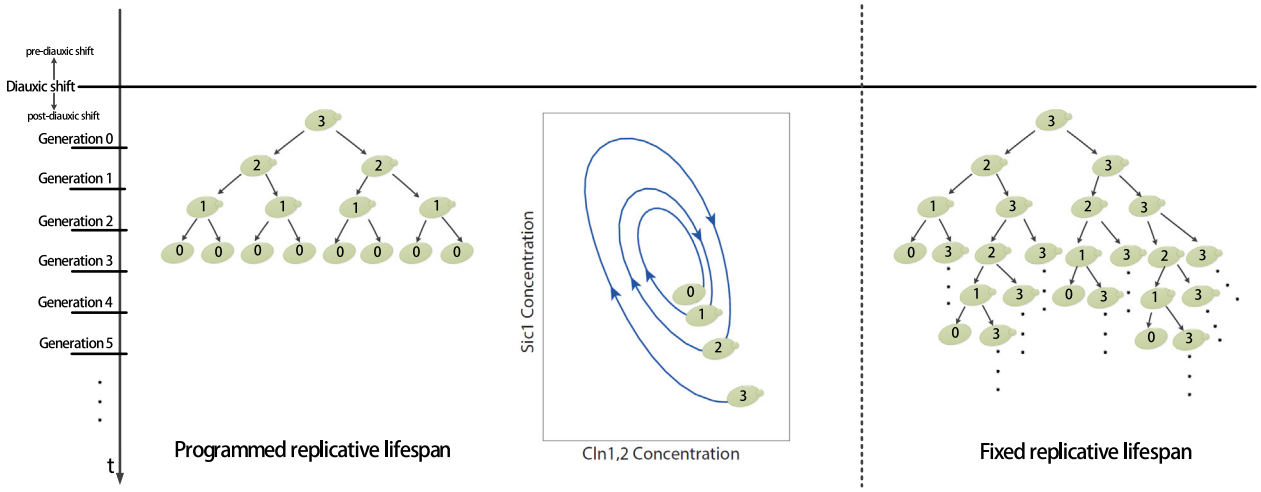

Fig. 1. Programmed replicative lifespan versus fixed replicative lifespan. The number drawn on each cell represents its dividing potential, recording the number of oscillating times left. When this number is zero, the cell stops doubling. In the left panel, a mother cell has the capacity of dividing three times. After doubling once, its dividing potential reduces to 2 (left path). As shown in the middle panel, after going around the cell cycle once, the expression level of the genes/proteins such as Sic2 and Cln1,2 in the mother cell reaches a state with a capacity of dividing two times. A daughter (right path) born at this time inherits the gene expression and protein activation levels with its mother. Therefore, it can divide two times. In comparison, a different choice is that each daughter cell has a fixed dividing potential. In the right panel, each cell can divide three times. These two hypotheses will lead to distinct growth curves.

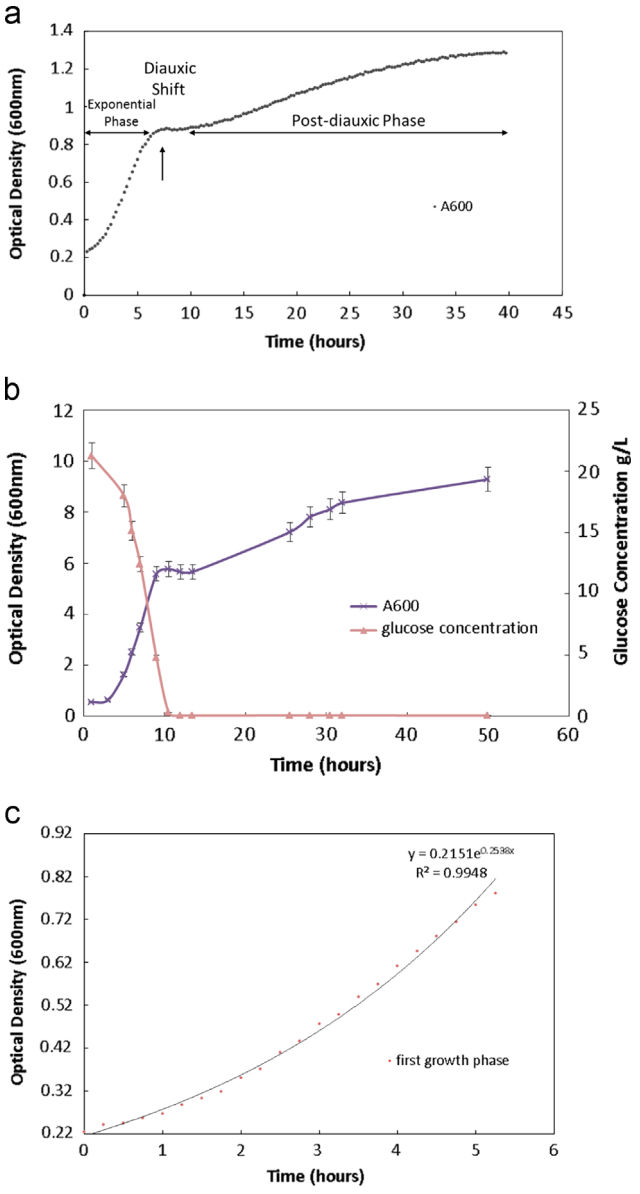

Fig. 2. Growth curves of *S. cerevisiae* BY4743 in YPD media. (a) Culture density. The data are measured by scattering at 600 nm and by a Fully Automatic Growth Curve Analyzer, every 15 min (see Section 3). From the time scale of this curve, the arrow place indicates the time point of which cells enter the diauxic shift at about the sixth hour. (b) Culture density and residual glucose concentrations. The data are measured by an ultraviolet spectrophotometer at 600 nm (time interval can be seen in Section 3). The glucose is exhausted at about 10 h. (c) The exponential growth phase (measured by a Fully Automatic Growth Curve Analyzer) before the diauxic shift is calculated by fitting an exponential curve to the experimental data and represented by a solid line, the coefficient of determination $R^2 = 0.9948$.

integer less than or equal to $T_s/\Delta T$; $\sum_i \rho_i = N_0$. The daughter cell has the capability of dividing as well, but the number of dividing is reduced to the times left of the mother cell. As an example from Fig. 1, for a mother cell that can divide three times, a daughter cell born at generation 1 can divide two times. If all cells start doubling at the same time $t=0$, we can write down the total number of yeast at time t

$$N(t) = \sum_{i=0}^{[T_s/\Delta T]} \rho_i \left[1 + \sum_{j=0}^{[t/\Delta T]-1} 2^j \theta(i-j)\right] = \sum_{i=0}^{[T_s/\Delta T]} 2^{\min\{[t/\Delta T], i\}} \rho_i \qquad (1)$$

here $\theta(i-j)$ is the unit step function: $i \le j$, $\theta(i-j)=0$ and $i>j$, $\theta(i-j)=1$. In practice, the cells are usually not synchronized, we cannot assume that they begin replicating simultaneously. Taking into account of this, the discrete distribution function ρ_i is replaced by a continuous function of time $\rho(t)$. When cell number is large enough, we can use a continuous approximation and obtain a continuous model:

$$N(t) = N_0 C \int_0^{T_s} dt_1 \int_0^t dt_2 \left[\rho(t_1)\left(2^{t_2/\Delta T}\right)\theta(t_1 - t_2)\right] \qquad (2)$$

where C is the normalization constant generated by the continuous approximation; $\rho(t)$ is the distribution of yeast with different dividing capacities.

We can obtain a growth curve from Eq. (2) with an initial population distribution $\rho(t)$ drawn on the left panel of Fig. 3, it is consistent with the experimental data, see the right panel of Fig. 3. We will further show in the following that these two programs can be implemented by the endogenous molecular-cellular network of yeast. The combined theoretical results of both exponential growth and post diauxic growth comparing with the experimental data are shown in Fig. 4.

2.2. A network model of cell cycle

This endogenous molecular-cellular network exists in yeast, which is a highly conserved, robust, nonlinear and stochastic dynamical system (Zhu et al., 2004; Ao et al., 2008; Wang et al., 2013). Generally, it consists of transcription factor network, and signal transduction pathway, including key factors or modules like cell cycle and stress response. In this section, we construct an endogenous network in order to demonstrate our hypothesis that the different yeast growth modes are determined by the molecular-cellular network.

Our network consists of two parts: the cell cycle part and the pheromone responsive part of MAPK. The cell cycle part is highly conserved in eucaryotic organisms including mammalian cells. It controls the growth of a single cell (Zhu et al., 2000), and is closely related to yeast replicative lifespan. We use five cell cycle controlled regulators, Cln3, Swi6, Cln1,2, Sic1, and Swe1, to construct the cycle part. The MAPK pathway can remarkably influence the yeast growth (Dohlman and Thorner, 2001).

In the exponential growth phase, the cell cycle part alone drives the network oscillating persistently as in Fig. 5(a), reflecting the infinite replicative capacity. We provide an intuitive explanation about how the cycle part oscillates. We start with a high initial concentration of Sic1. This protein can indirectly activate the start cyclin-dependent kinase, Cdc28/Cln3, which can trigger the cell cycle from the G1 to S. Once Cdc28/Cln3 is active, it will activate Swi6 and Cln1,2 successively. At this time, Swe1, which is a inhibitor activated by Swi6, plays a role to suppress Cln3 and Cln1,2.

The second is the pheromone responsive part of the MAPK pathway. Yeast growth is remarkably influenced by pheromone. The signal of pheromone propagates along the pathway, finally adjusts the gene expression level. In our model, we use the gene *Far1* to function on the cell cycle network, because *Far1* is on the MAPK signaling pathway, and it inhibits Cdc28/Cln1,2 and Cdc28/Cln3 (Dohlman and Thorner, 2001; Mendenhall and Hodge, 1998). Conversely, the cell cycle can feedback to the MAPK pathway on Ste5 (Strickfaden et al., 2007). After the second part is activated by pheromone, the cell cycle is inhibited, and gradually stops. The total oscillating time is determined by the initial gene expression level.

3. Materials and methods

3.1. Strain and media

The yeast strain used in this work is BY4743 (*MATa*/*α*; *his*3Δ1/*his*3Δ1; *leu*2Δ0/*leu*2Δ0; *LYS*2/*lys*2Δ0; *met*15Δ0/*MET*15; *ura*3Δ0

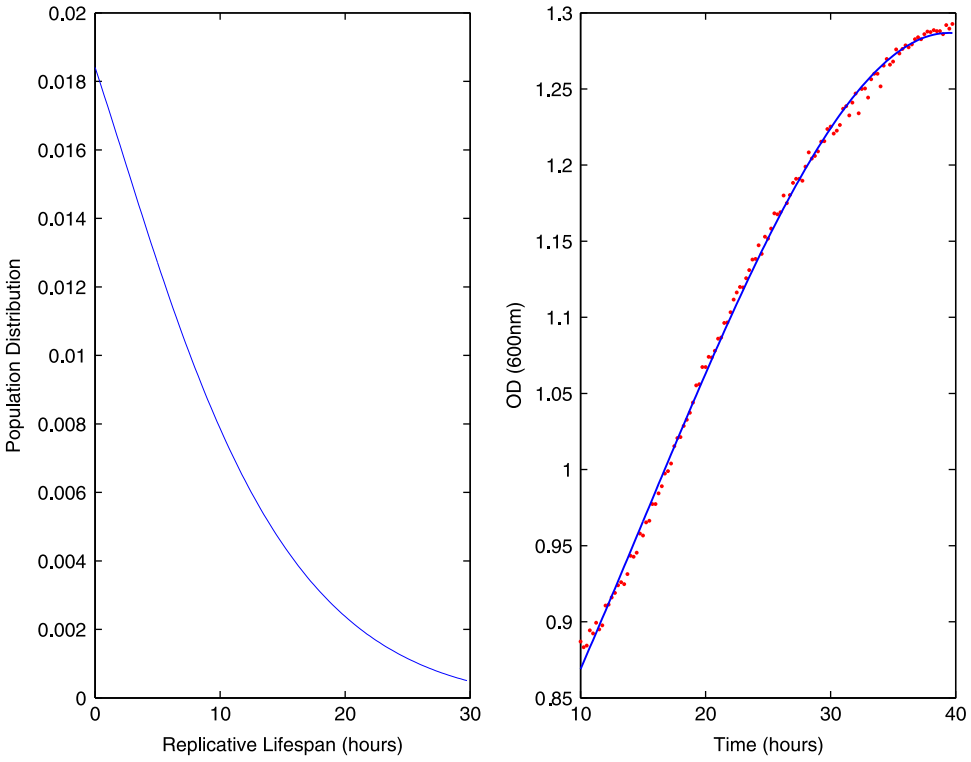

Fig. 3. (color online) Experimental data versus calculational result. Left panel: The initial population distribution of the mother cells $\rho(t)$. Right panel: Experimental data are denoted by the red dots. Calculational result obtained from Eq. (2) with the initial distribution $\rho(t)$ in the left panel is drawn by the blue line.

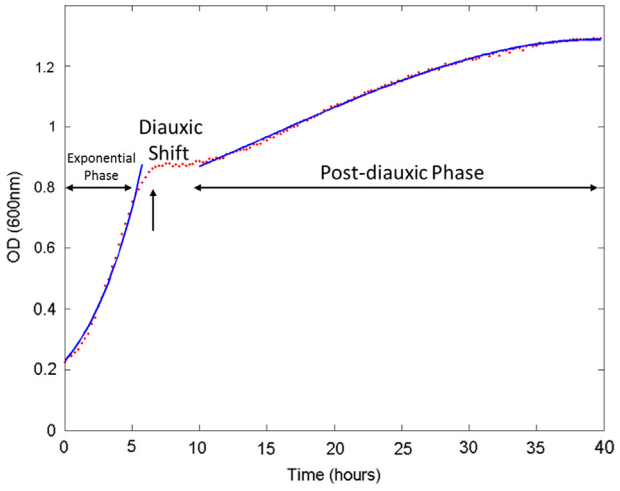

Fig. 4. (color online) Theoretical calculated curves versus experimental data: The blue lines denote the theoretically obtained growth curves in the exponential phase and the post-diauxic growth phase. The red dots are experimentally measured data (see also Fig. 2).

/*ura*3Δ0). YPD (yeast extract 1%, peptone 2%, and glucose 2%, from Sangon Biotech.) medium is used to perform batch culture.

3.2. Growth stage analysis

A growth curve experiment is performed by inoculating yeast cells from an overnight culture in YPD medium by diluting 1:10 into 100 ml of fresh YPD medium. The initial value of optical density at 600 nm (OD_{600}) is around 0.5 ($OD_{600}=0.5$; corresponding to 10^7 cells/ml). Samples are removed to 100-well plate (Bioscreen Honey-comb, HC2 PAT.PEND, made in Finland), 100 μl/well. Then the plate is incubated in the Fully Automatic Growth Curve Analyzer (Bioscreen C, a computer-controlled shaker/incubator/reader instrument), at 28°C, by medium shaking. The optical density is measured at 600 nm every 15 min for 40 h.

Another approach is used to measure the culture density (Brauer et al., 2005). At each time-point (1, 3, 5, 6, 7, 9, 10.5, 12, 13.5, 25.5, 28, 30.5, 32, 50 h), 2 ml of sample is measured at absorbance of 600 nm by using the ultraviolet spectrophotometer (SHIMADZU, UV-1800, made in Japan) manually.

3.3. Glucose assay

At each time-point (1, 5, 6, 7, 9, 10.5, 12, 13.5, 25.5, 28, 30.5, 32, 50 h), 1 ml of culture broth is centrifuged for 2 min at 10 000 rpm. The pellet is discarded, and the supernatant is stored at −20 °C for glucose assay. Residual glucose in the growth medium (supernatant) is measured by enzyme-coupled NADH oxidation reactions (glucose assay kit from SIGMA-ALDRICH, GAHK20-1KT, made in USA) (Brauer et al., 2005).

3.4. Dynamics of the endogenous molecular-cellular network

In a mathematical model, the activating or inhibiting relation is expressed by the Michaelis–Menten equation (Murray, 2002). The gene expression and protein activation x is up regulated by activators and down regulated by inhibitors, together with a self-degradation part

$$\frac{dx}{dt}=-x+V_M\cdot\frac{A}{K+A}\cdot\frac{1}{K+I} \tag{3}$$

where K is the Michaelis constant, n is the Hill coefficient, V_M is the maximal synthesis rate, $A=A_1^n+\cdots+A_m^n$ consists of the activators of x, $I=I_1^n+\cdots+I_m^n$ consists of the inhibitors of gene x, $-x$ represents the self-degradation. In this way, we build the

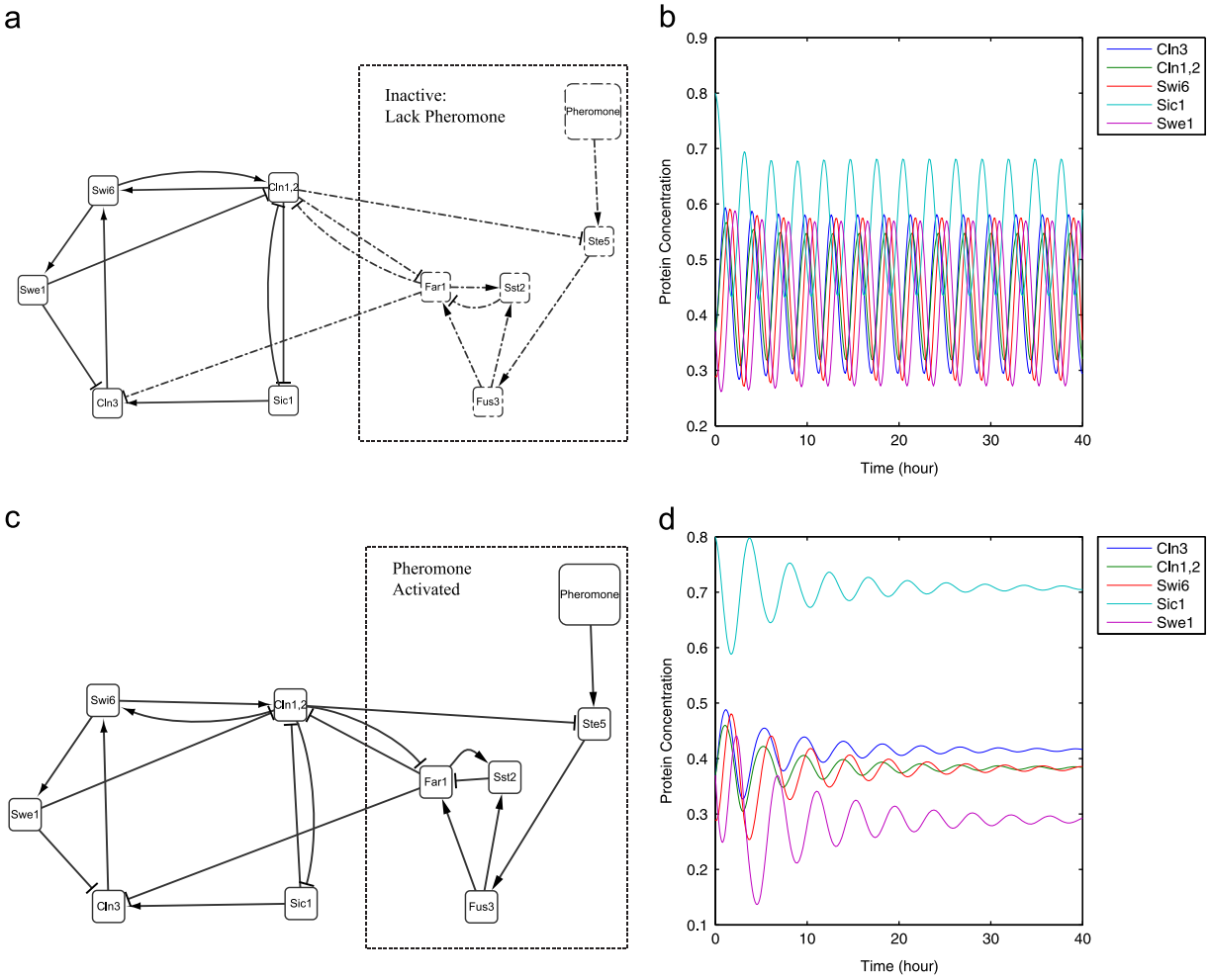

Fig. 5. Endogenous network model: The network is displayed in (a) and (c) for the exponential growth and the post-diauxic growth respectively. We emphasis that the two phases are formed by a common network. However, the pheromone responsive part of the MAPK pathway plays different roles in cooperation with the cell cycle. The dynamics of (a) has a limit cycle attractor. After pheromone activates the MAPK pathway, the limit cycle attractor is replaced by a fixed point attractor in (c). We show the simulation results of corresponding dynamical models in (b) and (d). In (b) the model oscillates permanently indicating an infinite replicative lifespan; in (d) the model oscillates finite times and depends on its initial condition, indicating a finite lifespan.

dynamical mathematical model of the network as follows:

$$
\begin{aligned}
\dot{x}_1 &= -x_1 + V_M \cdot \frac{x_4^n}{1+K\cdot x_4^n} \cdot \frac{1}{1+K\cdot(x_5^n+\alpha\cdot x_6^n)}\\
\dot{x}_2 &= -x_2 + V_M \cdot \frac{x_3^n+\beta\cdot x_4^n}{1+K\cdot(x_3^n+\beta\cdot x_4^n)} \cdot \frac{1}{1+K\cdot(x_5^n+\alpha\cdot x_6^n)}\\
\dot{x}_3 &= -x_3 + V_M \cdot \frac{x_1^n}{1+K\cdot x_1^n}\\
\dot{x}_4 &= -x_4 + \frac{1}{1+K\cdot x_2^n}\\
\dot{x}_5 &= -x_5 + V_M \cdot \frac{x_3^n}{1+K\cdot x_3^n}\\
\dot{x}_6 &= -x_6 + V_M \cdot \frac{x_8^n}{1+K\cdot x_8^n} \cdot \frac{1}{1+K\cdot(x_2^n+x_7^n)}\\
\dot{x}_7 &= -x_7 + V_M \cdot \frac{x_6^n}{1+K\cdot x_6^n}\\
\dot{x}_8 &= -x_8 + V_M \cdot \frac{x_9^n}{1+K\cdot x_9^n}\\
\dot{x}_9 &= -x_9 + P \cdot \frac{1}{1+K\cdot\gamma\cdot x_2^n}
\end{aligned}
$$

where P represents the amount of pheromone ($P=0$ corresponds to the exponential phase, $P=1$ corresponds to the post-diauxic phase); $V_M=50$, $K=50$, $n=5$; $\alpha=1.3$, $\beta=0.5$, $\gamma=0.1$ represent the relative interaction strength; the variables $x_1 \to x_9$ represent gene expression and protein activation of *Cln3*, *Cln1/2*, *Swi6*, *Sic1*, *Swe1*, *Far1*, *Sst2*, *Fus3*, *Ste5*. Pheromone is regarded as a parameter which is different in the two modes of yeast growth.

We show the simulation results with low pheromone value and high pheromone value in Fig. 5(a) and (d). In Fig. 5(b), the model oscillates permanently indicating an infinite replicative lifespan; in Fig. 5(d), the model oscillates finite times and depends on its initial condition, indicating a finite lifespan.

4. Conclusion

Cell cycles are highly conserved in most eukaryotic cells. For this reason, *S. cerevisiae* is traditionally used as a model organism to study the cell cycle. From our theoretical model, the exponential growth of yeast is associated with a limit cycle attractor of its endogenous molecular network dynamics. The post-diauxic growth corresponds to a fixed point attractor. The change of dynamical behavior is a result of the activation of the pheromone responsive mitogen-activated protein kinase pathway. To verify, we calculate the curves of the two growth phases. They are consistent with the experimental data. In yeast, while Far1 inhibits proliferation, a crosstalk with factors such as Ste13, Kss1, Tec1, and PKA may complicate outcomes. Our study suggests that complication may arise from both molecular interaction and inherited gene/protein profiles passing through generations. This may turn out to be an important direction for future research because it implies that replicative capacity may be intervened by targeting

molecular levels in addition to or instead of changing molecular interaction strength.

Acknowledgments

This work was supported in part by the National 973 Project no. 2010CB529200; by the Natural Science Foundation of China (No. NSFC91029738); and by the grants from the State Key Laboratory of Oncogenes and Related Genes (No. 90-10-11).

References

Allsopp, R.C., Vaziri, H., Patterson, C., Goldstein, S., Younglai, E.V., Futcher, A.B., Greider, C.W., Harley, C.B., 1992. Telomere length predicts replicative capacity of human fibroblasts. Proc. Natl. Acad. Sci. U. S. A. 89 (21), 10114–10118.

Ao, P., Galas, D., Hood, L., Zhu, X.-M., 2008. Cancer as robust intrinsic state of endogenous molecular-cellular network shaped by volution. Med. Hypotheses 70 (3), 678–684.

Ball, D.A., Marchand, J., Poulet, M., Baumann, W.T., Chen, K.C., Tyson, J.J., Peccoud, J., 2011. Oscillatory dynamics of cell cycle proteins in single yeast cells analyzed by imaging cytometry. PloS One 6 (10), e26272.

Blagosklonny, M.V., Hall, M.N., 2009. Growth and aging: a common molecular mechanism. Aging 1 (4), 357–362.

Bodnar, A.G., Ouellette, M., Frolkis, M., Holt, S.E., Chiu, C.-P., Morin, G.B., Harley, C.B., Shay, J.W., Lichtsteiner, S., Wright, W.E., 1998. Extension of life-span by introduction of telomerase into normal human cells. Science 279 (5349), 349–352.

Brauer, M.J., Saldanha, A.J., Dolinski, K., Botstein, D., 2005. Homeostatic adjustment and metabolic remodeling in glucose-limited yeast cultures. Mol. Biol. Cell 16 (5), 2503–2517.

Broach, J.R., 2012. Nutritional control of growth and development in yeast. Genetics 192 (1), 73–105.

Dohlman, H.G., Thorner, J., 2001. Regulation of G protein-initiated signal transduction in yeast: paradigms and principles. Annu. Rev. Biochem. 70 (1), 703–754.

Hayflick, L., 1965. The limited in vitro lifetime of human diploid cell strains. Exp. Cell Res. 37 (3), 614–636.

Herker, E., Jungwirth, H., Lehmann, K.A., Maldener, C., Fröhlich, K.-U., Wissing, S., Büttner, S., Fehr, M., Sigrist, S., Madeo, F., 2004. Chronological aging leads to apoptosis in yeast. J. Cell Biol. 164 (4), 501–507.

Kuchler, K., Sterne, R.E., Thorner, J., 1989. *Saccharomyces cerevisiae* STE6 gene product: a novel pathway for protein export in eukaryotic cells. EMBO J. 8 (13), 3973–3984.

Kurjan, J., 1992. Pheromone response in yeast. Annu. Rev. Biochem. 61 (1), 1097–1129.

Lamersdorf, N.P., Borken, W., 2004. Clean rain promotes fine root growth and soil respiration in a Norway spruce forest. Global Change Biol. 10 (8), 1351–1362.

Lawless, C., Jurk, D., Gillespie, C.S., Shanley, D., Saretzki, G., von Zglinicki, T., Passos, J. F., 2012. A stochastic step model of replicative senescence explains ROS production rate in ageing cell populations. PloS One 7 (2), e32117.

Lundblad, V., Szostak, J.W., 1989. A mutant with a defect in telomere elongation leads to senescence in yeast. Cell 57 (4), 633–643.

Mendenhall, M.D., Hodge, A.E., 1998. Regulation of Cdc28 cyclin-dependent protein kinase activity during the cell cycle of the yeast *Saccharomyces cerevisiae*. Microbiol. Mol. Biol. Rev. 62 (4), 1191–1243.

Monod, J., 1949. The growth of bacterial cultures. Annu. Rev. Microbiol. 3 (1), 371–394.

Mortimer, R.K., Johnston, J.R., 1959. Life span of individual yeast cells. Nature 183, 1751–1752.

Murray, J.D., 2002. Mathematical Biology: I. An introduction, 3rd ed., vol. 2. Springer-Verlag, New York.

Stahl, G., Salem, S.N.B., Chen, L.-F., Zhao, B., Farabaugh, P.J., 2004. Translational accuracy during exponential, postdiauxic, and stationary growth phases in *Saccharomyces cerevisiae*. Eukaryot. Cell 3 (2), 331–338.

Strickfaden, S.C., Winters, M.J., Ben-Ari, G., Lamson, R.E., Tyers, M., Pryciak, P., 2007. A mechanism for cell-cycle regulation of MAP kinase signaling in a yeast differentiation pathway. Cell 128 (3), 519–531.

Suda, Y., Suzuki, M., Ikawa, Y., Aizawa, S., 1987. Mouse embryonic stem cells exhibit indefinite proliferative potential. J. Cell. Physiol. 133 (1), 197–201.

Wagner, W., Horn, P., Castoldi, M., Diehlmann, A., Bork, S., Saffrich, R., Benes, V., Blake, J., Pfister, S., Eckstein, V., et al., 2008. Replicative senescence of mesenchymal stem cells: a continuous and organized process. PloS One 3 (5), e2213.

Wang, G.-W., Zhu, X.-M., Hood, L., Ao, P., 2013. From Phage lambda to human cancer: endogenous molecular-cellular network hypothesis. Quant. Biol. 1, 32–49.

Zeng, X., Rao, M.-S., 2007. Human embryonic stem cells: long term stability, absence of senescence and a potential cell source for neural replacement. Neuroscience 145 (4), 1348–1358.

Zhu, G.-F., Spellman, P.T., Volpe, T., Brown, P.O., Botstein, D., Davis, T.N., Futcher, B., 2000. Two yeast forkhead genes regulate the cell cycle and pseudohyphal growth. Nature 406 (6791), 90–94.

Zhu, X.-M., Yin, L., Hood, L., Ao, P., 2004. Calculating biological behaviors of epigenetic states in the phage λ life cycle. Funct. Integr. Genomics 4 (3), 188–195.